JOURNAL OF MATERIALS SCIENCE 2 (1967) 18–27

Structural Features of Pyrolytic Graphite

T. HIRAI, S. YAJIMA
The Research Institute for Iron, Steel and Other Metals, Tôhoku University, Sendai, Japan

Received 26 July 1966

The structure of pyrolytic graphite has been examined on several samples deposited under various conditions at 1340 to 2310° C and 5 to 200 torr by means of an X-ray technique. The structural features investigated include interlayer spacing, ordering, preferred orientation, intercrystallite porosity, and crystallite size. These features are closely related to the microstructure and density. In particular, the temperature dependence of crystallite size explains three types of formation mechanism, the cause of the occurrence of a minimum density at a certain temperature, and the cause of a preferred orientation in pyrolytic graphite.

1. Introduction

In recent years, a considerable amount of research has been concerned with materials for high-temperature and nuclear applications. Pyrolytic graphite of a high degree of anisotropy, prepared by pyrolysis of a hydrocarbon gas at temperatures above about 2000° C, is used as a material for high-temperature thermal insulators, including special crucibles and induction susceptors [10, 18], while pyrolytic carbon of low anisotropy, prepared below about 1600° C, is employed as the coating material for nuclear fuel particles (as in the "Dragon" reactor). It is well known that thermal and electrical anisotropy originate in features of the crystal structures such as interlayer spacing, ordering between the layers, preferred orientation, and crystallite size. Investigations of such aspects of crystal structures have been reported, but no clear account has been given of their mutual structural correlations and the relations between the structural features and conditions of preparation of pyrolytic graphite.

In previous papers [1, 2], it has already been made clear that the formation mechanism, microstructure, and density depend on the conditions of preparation, particularly the deposition temperature and gas pressure, and that the mechanism of formation is related to the microstructure and density. In the present study, the effects of the deposition temperature and gas pressure on the crystal structures and the relations of the crystal structures with the formation mechanism, microstructure, and density have been investigated.

2. Experimental Procedures

Pyrolytic graphite was prepared by pyrolysis of propane gas, dried with calcium chloride and phosphorus pentoxide, by direct heating of the substrate (direct heating method). The conditions of preparation were as follows: the deposition temperatures, 1340 to 2310° C; gas pressures, 5 to 200 torr; flow rate, 640 cm^3/min. The processes have been fully described elsewhere [1].

X-ray measurements were made using a diffractometric unit and by means of Ni-filtered CuKα radiation. In some cases, the diffractometer was used as a single-crystal unit, and the specimens were mounted on a single-crystal orienter which permitted controlled changes of the specimen orientation relative to the incident and diffracted X-ray beams. The values of the average interlayer spacings were obtained from the (002) and (004) lines of diffraction patterns of the powdered samples (325 mesh). The (002) reflections were not corrected for the polarisation and absorption factors. Mainly the (004) reflections were used for the determination of the interlayer spacing, because there was practically no need to correct the (004) reflections [3]. The values obtained from the (002) reflections were used for reference only, in case

the intensity of the (004) reflections was unmanageably low. Ordering was determined qualitatively from the line shapes of the two-dimensional (10) reflections. Block and flat specimens were also examined in transmission.

The specimens used for measurements of the preferred orientation were 0.2 to 0.3 mm-square rods with a length of about 10 mm. Since only 30 to 50% of X-rays is absorbed in such specimens, the non-circularity of the cross-section could be disregarded. The specimens were mounted as shown in fig. 1, and the measurements were made on the (002) reflections. The

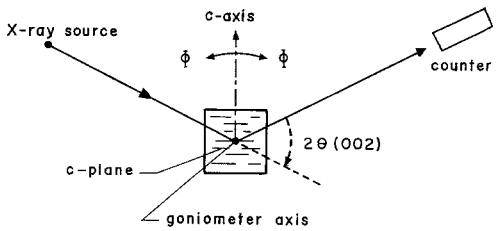

Figure 1 X-ray measurement of preferred orientation.

angle of 2θ was fixed at the position of maximum intensity of the (002) reflections, by rotating the specimens and the counter; during the measurements only the specimens were rotated about the goniometer axis, while the counter was kept stationary. The (002) reflections were traced at varying angles of the specimen rotation about the axis parallel to the deposition plane. The data presented here have been normalised to $I\ (002)_{\max} = 1$. In comparing the results of preferred orientation measurements of different specimens, an anisotropy factor (σ_{oz}/σ_{ox}) is adopted [4]. If the curves of I (002) versus Φ fit the function $|\cos^n\Phi|$, the *anisotropy factor* is represented by $(n + 1)$. Crystallite sizes of L_a and L_c were determined from the half-width of the (110) reflection in the transmitting position, and the (002) reflection in the reflecting position, respectively. In the transmission method, the half-width of the (110) reflection was considerably affected by the thickness x of the specimen which affects the X-ray transmission, so that the correction for this was made and the thickness normalised to $x = 1.5$ mm [5]. Although a considerable amount of strain effect exists in the half-width of the (002) reflection [6], the apparent crystallite size was estimated from the half-width without correcting for this effect.

3. Experimental Results

3.1. Interlayer Spacing ($c_0/2$) and Intercrystallite Porosity (*ip*)

The effects of temperature on the interlayer spacing at 5 to 100 torr are shown in figs. 2a to 2d. In fig. 2a, the relation at 5 torr is given. In the temperature range 1535 to 2215° C, the interlayer spacing is constant ($c_0 \approx 6.847$ Å). As shown in fig. 2b, the interlayer spacing depends strongly on the temperature at 10 torr. The value of c_0 (002) is as large as 7.045 Å at 1535° C and decreases rapidly to about 6.88 Å as the temperature is raised to 1635° C. Above 1635° C, c_0 (004) decreases linearly with increasing temperature. At 50 torr, c_0 (002) shows a maximum value at 1730° C, as shown in fig. 2c. Fig. 2d shows the relation at 100 torr. In the temperature range 1535 to 1830° C, c_0 (004) is constant (about 6.85 Å), independent of temperature. Above 1830° C, it decreases as the temperature is increased. As shown in figs. 2a to 2d, the relations between interlayer spacing and temperature are very complex, and the effect of temperature markedly varies with pressure.

Fig. 3 shows the relations between four microstructures [2] and interlayer spacing. At 5 torr, the structures "C" and "F"* are obtained at low and high temperatures respectively, but the interlayer spacing is constant and is independent of changes in the microstructure. At 10, 50, and 100 torr, the structure "F" is obtained in the phase in which the interlayer spacing decreases with increasing temperature, while the structures "C", "P" and "S" are observed in the phase showing an abnormal behaviour of the interlayer spacing with temperature. The calculated density (d) is obtained from the experimental interlayer spacing (c_0). The value of d is calculated from c_0 obtained from the smooth curves shown in figs. 2a to 2d. Fig. 4 shows d and the experimental density (D) at 50 torr, with a solid line and a dotted line respectively. As shown in fig. 4, D depends largely on temperature and reaches a minimum value at about 1740° C. However, d is almost independent of temperature. To compare the difference between d and D, the intercrystallite porosity (*ip*) is defined as follows:

$$ip = (d - D)/d \times 100\ (\%)$$

The relation of *ip* with temperature is shown in

*The names of the four morphological types "F", "S", "C", and "P" are listed below fig. 3; these structures are described in detail in reference 2.

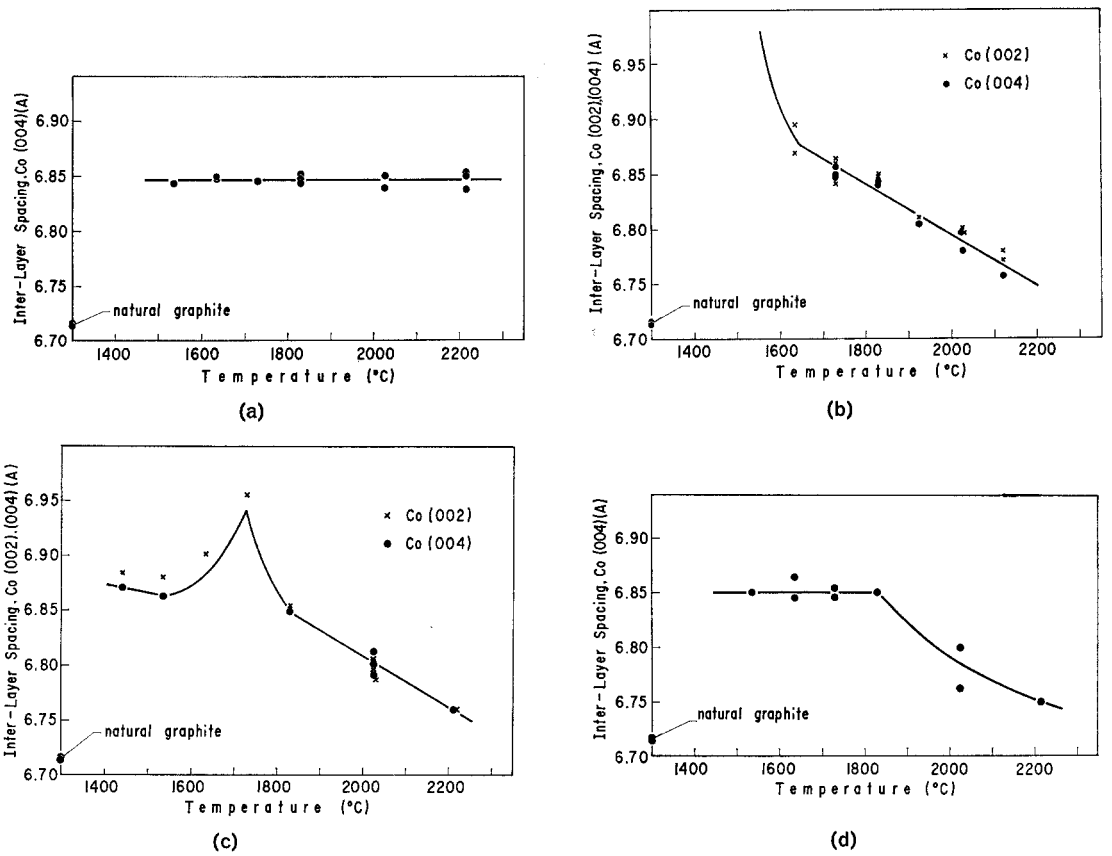

Figure 2 Temperature effect on the interlayer spacing at: (a) 5 torr; (b) 10 torr; (c) 50 torr; (d) 100 torr.

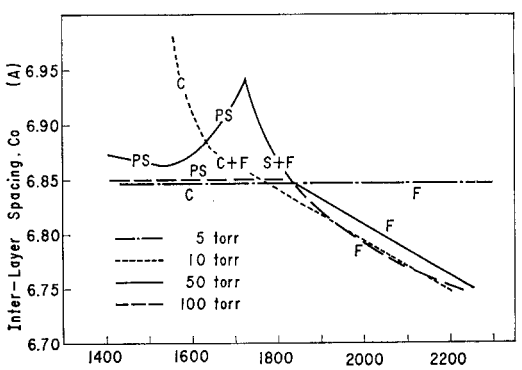

Figure 3 The relation between interlayer spacing and microstructure. (F : fine regenerative structure; S : string structure; C : coarse structure; P : pebble structure.)

fig. 5. The value of *ip* is a few per cent, above about 1700° C and with a low pressure of 5 and 10 torr, and above about 2000° C and with a high pressure of 50 and 100 torr. However, *ip* reaches about 45% at the temperature at which a minimum density is obtained (10 torr).

3.2. Ordering

The transition from complete disorder to complete order is reflected in the change in the (*hk*)-band shape. For complete order, the two-dimensional (10) reflection is split into the crystalline (100), (101), and (102) reflections. Figs. 6a and 6b show the (10) reflections of the

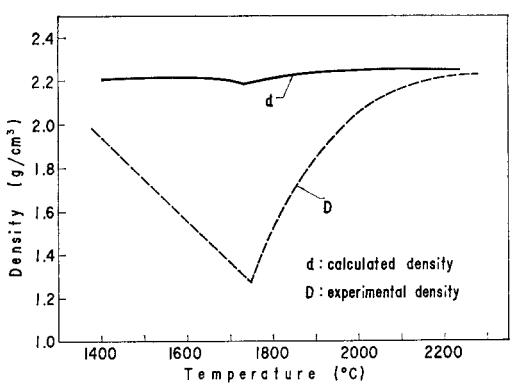

Figure 4 The calculated density (*d*) and experimental density (*D*) at 50 torr.

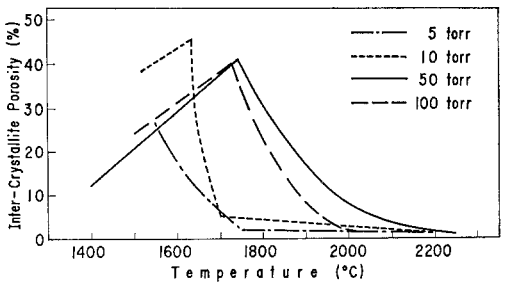

Figure 5 Effects of conditions of preparation on the inter-crystallite porosity.

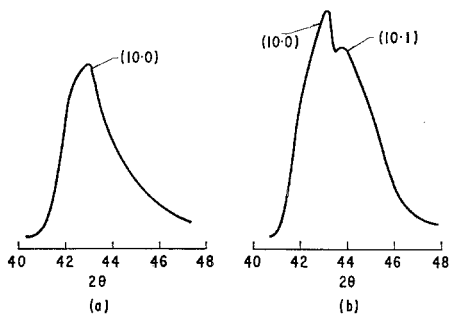

Figure 6 The (10) reflections of the deposits with no ordering (a) and ordering (b).

completely layer-disordered and partially layer-ordered materials respectively. In the present study, the amount of ordering was estimated qualitatively by comparing the (10) reflections, and was divided into four grades. The amount of ordering shown in fig. 6a is graded as "non" and that in fig. 6b as "strong", and that between them as "weak" and "medium". The effects of temperature and pressure on the ordering are shown in fig. 7. The amount of ordering increased remarkably as the temperature and pressure were raised. As shown in fig. 7 with the dotted lines, the amount of ordering was closely related to the microstructures classified by the authors [2]. The ordering was not observed in the structures "S" and "P" obtained at low temperatures and high pressures, nor in the structure "C" at low temperatures and low pressures, but was observed only in the structure "F", except for that obtained at 5 torr.

3.3. Preferred Orientation

A representative result of the preferred orientation measurement is shown in fig. 8. The effects of temperature and pressure on the anisotropy factor are shown in fig. 9. The anisotropy factor of pyrolytic graphite obtained

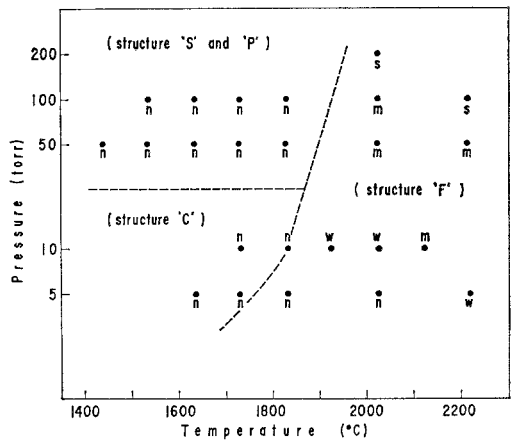

Figure 7 Effects of conditions of preparation on the ordering. (s : strong; m : medium; w: weak; n : none.)

at low temperatures is generally small, and becomes remarkably lower for high gas pressure. At 5 and 10 torr, the anisotropy factors are practically independent of the microstructural change from "C" to "F". At 50 and 100 torr, however, there are marked changes in the anisotropy factor in line with the microstructural change from "P" and "S" to "F". The anisotropy factor increases in the region of "P" and "S" with increasing temperature, but it is practically constant in the region of "F", independent of temperature. In fig. 9, ⊗ and ⊙ show the anisotropy factor of the deposits containing the heteromorphic phase of the laminar type [2].

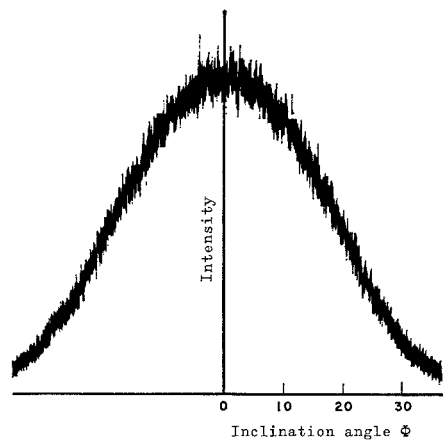

Figure 8 Typical preferred orientation diffraction traverse.

3.4. Crystallite Size

The effects of temperature on L_a and L_c at 5 to 100 torr are shown in figs. 10a to 10d In fig. 10a,

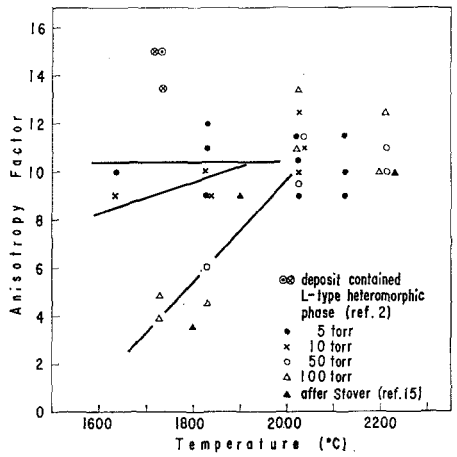

Figure 9 Effects of conditions of preparation on the anisotropy factor.

the relation at 5 torr is given. The value of L_a increases slightly with temperature. In the temperature range of 1635 to 1730° C, L_c increases with temperature. Above this temperature range, L_c is independent of the temperature and shows a constant value of about 180 Å. Fig. 10b shows the relation at 10 torr. The value of L_a is nearly constant (about 74 Å) in the temperature range of 1340 to 1635° C, but it increases abruptly above this temperature range. The relation of log L_a as a function of temperature is linear. At low temperatures below about 1600° C, it seems that L_c is nearly constant (about 60 Å), but this behaviour is not clear owing to the error in the measurements of the half-width of the reflections. In the temperature range from about 1600 to 1750° C, L_c increases

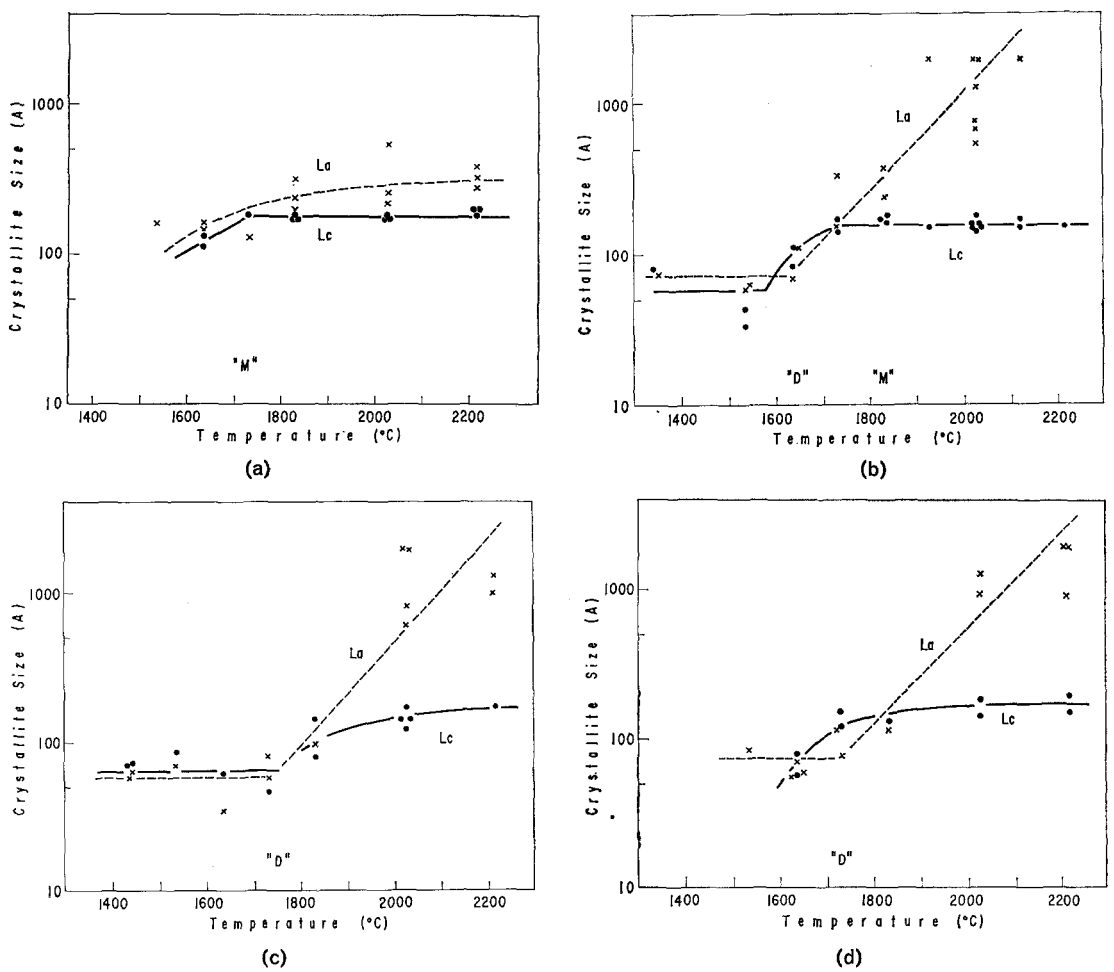

Figure 10 Temperature effects on the crystallite sizes at: (a) 5 torr (a minimum density does not appear in this condition); (b) 10 torr; (c) 50 torr (the change in the mechanism of formation does not appear in this condition); (d) 100 torr (the change in the mechanism of formation does not appear in this condition).

rapidly with temperature. Above about 1750° C, L_c is independent of temperature and shows a constant value of about 150 Å. This behaviour is similar to that at 5 torr. Fig. 10c shows the relation at 50 torr. In the temperature range 1440 to 1750° C, L_a is nearly constant (about 60 Å). Above about 1750° C, the relation of log L_a versus temperature is similar to that at 10 torr. The temperature dependence of L_c also resembles that at 10 torr in the low-temperature range. In the high-temperature range, L_c increases with temperature. As shown in fig. 10d, the relations of temperature versus log L_a and L_c at 100 torr are similar to those at 50 torr. The two curves of L_c obtained at 50 and 100 torr shown in figs. 10c and 10d have essentially the same shape. However, the temperature at which the increase of L_c begins at 100 torr is about 100° C lower than that at 50 torr. These results are closely related to the mechanism of pyrolytic graphite formation and the appearance of a minimum density.

4. Discussion

4.1. Interlayer Spacing and Intercrystallite Porosity

In pyrolytic graphite prepared by a direct heating method, several properties of the part which is in contact with the substrate are known to be different from those in the surface layer [7-10]. In this study, however, measurements were made to assess the structure of an entire block. Guentert [6] obtained pyrolytic graphite at 1700 to 2500° C in a resistance-heated furnace (R: indirect heating method) and reported that the measured values of $c_0/2$ were between 3.416 and 3.433 Å. Guentert and Prewitt [11] measured the values to be 3.43 and 3.35 Å at 1700 and 2500° C respectively. Although the gas pressures used in their experiments are unknown in detail, the results are in good agreement with the present results obtained at 5 (fig. 2a) and 10 torr (fig. 2b) respectively. Blackman *et al* [12] prepared pyrolytic graphite by cracking methane on a graphite substrate heated in the temperature range 1600 to 2200° C at high pressures (direct heating method). Their results are similar to those obtained at 100 torr in this work, as shown in fig. 2d. The effect of temperature on the interlayer spacing is too complex to make clear in this experiment. In the previous paper [2], it has been reported that a minimum density has been observed at about 1700° C and 10 to 100 torr. However, the density (d) calculated from c_0 is about 2.2 g/cm³ over the whole temperature range. Therefore, the cause of the decrease in density may be attributed to the intercrystallite pore, not to the change in c_0. Bragg *et al* [13] examined the small-angle scattering from pyrolytic graphite obtained at 2100° C (2.19 g/cm³), and reported that the scattering was due to the presence of microvoids which were nearly as numerous as the crystallites in pyrolytic graphite, and were probably pyramidal crevices. Stiegler [14] observed the structural features of pyrolytic carbon deposited on fuel particles in a fluidised bed at 1400 to 1800° C and reported that, by means of direct transmission microscopy of the cleaved flakes, the low-density deposits were shown to contain microvoids about 100 Å in diameter. If the number of the voids equals that of the crystallites, L_a and L_c are about 100 Å, so that the size of voids is about 90 Å in the case of $ip = 45\%$ (1.20 g/cm³), which is obtained at 1650° C and 10 torr in the present experiment. This is in good agreement with Stiegler's results.

4.2. Ordering

Guentert [6] obtained the (10) reflections of pyrolytic graphite deposited in the temperature range about 1700 to 2500° C in induction-heated (I: direct heating method) and resistance-heated (R: indirect heating method) furnaces. The amounts of ordering in Guentert's results of the I-samples may be graded as "weak" at 1900° C, "medium" at 2250° C, and "strong" at 2400° C, and those of all the R-samples as "non". He explained that the difference in the band shape of the I- and R-samples was due to the different amount of heat treatment allowed during the deposition. However, it does not always follow that the difference depends on this heat-treatment effect. Thus, in spite of similar heat treatments at 5 and 10 torr, at 10 torr the ordering is observed in the deposit obtained at temperatures above 1925° C, but at 5 torr it is slightly observed only above 2215° C, as shown in fig. 7. On the other hand, as the amount of ordering is said to have close bearing upon the value of c_0, it can be estimated from fig. 2 that the amount of ordering at 5 torr is a little smaller than that at 10 torr. This estimate corresponds to the results of observation of the (10)-band shape. Moreover, c_0 of the R-samples is in accord with that at 5 torr, and the amount of ordering corresponds to that at 10 torr. From the above considerations, it becomes evident that the difference between the amounts of ordering

of the I- and R-samples is caused by the variation of pressure used in the two methods rather than the different levels of heat treatment.

4.3. Preferred Orientation

The preferred orientation is markedly affected by temperature and pressure, as shown in fig. 9. The results of the anisotropy factor by Stover [15] are also shown, by the symbol ▲, in fig. 9. Although the condition for the preparation of pyrolytic graphite in his experiment is not known, it seems to have been carried out at high pressures, because the microstructures of the deposits correspond to those obtained at high pressures in our previous experiment [2], that is "S" at 1800° C and "F" at 1900 and 2000° C according to the authors' classification. Guentert [6] reported that in the temperature range 1700 to 1900° C the anisotropy factor of the R-sample increased rapidly with temperature, and, above 1900° C, it became nearly independent of temperature. The relation between density and temperature of the R-sample resembles that obtained in the present experiment at 100 torr. As already mentioned, from the values of the interlayer spacing and the amount of ordering, it has been predicted that the pressure for the preparation of the R-sample corresponds to 5 torr. These variations of the preferred orientation and density in the two methods are considered to be due to a greater contribution of the reaction process in the indirect heating method, which is more complex than that in the direct heating method.

4.4. Crystallite Sizes

The values of L_a and L_c of the R-sample by Guentert [11] and of pyrolytic graphite† measured by the authors are shown in fig. 11.

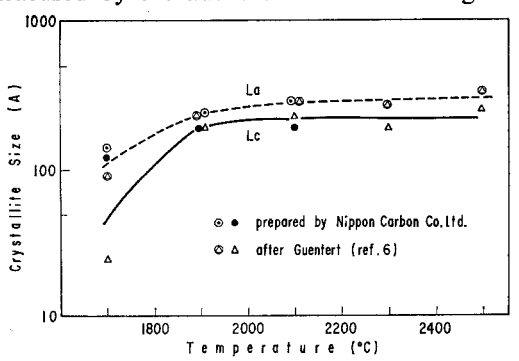

Figure 11 Temperature effects on the crystallite sizes in the indirect heating method.

These results are similar to that at 5 torr shown in fig. 10a. Brown *et al* [16] prepared pyrolytic graphite at 150 to 200 torr, and reported that the half-width of the (002) and (10) reflections showed a maximum value at 1600 to 1700° C and 1600° C respectively. Their results agree well with the present results, in that the temperature to begin the increase of L_c lowers as pressure is raised.

4.5. The Relation between Structural Features and Formation Mechanism of Pyrolytic Graphite

Comparing the present experimental results (in the direct heating method) with Guentert's (in the indirect heating method), the differences in both methods are revealed in the density and preferred orientation, but not in the ordering and the development of crystallite. These facts show that the manner of dehydrogenation and polymerisation in the vapour phase differ in the two methods. Bokros [17] investigated the relation between structural features and formation mechanism of carbons deposited at 1400° C in fluidised beds (indirect heating method). However, the preparation conditions adopted in his experiment differ very markedly from the present experiment, so that the present experimental results cannot be interpreted with his explanation.

As already reported [1], and as shown in fig. 12, there are three types of mechanism in the pyrolytic graphite formation by the direct heat-

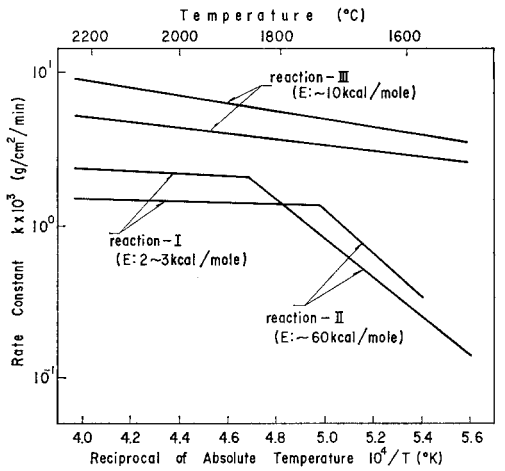

Figure 12 Arrhenius plot of the formation rate constants. (Reaction-I, II : low pressures; reaction-III : high pressures.)

†Prepared by Nippon Carbon Co Ltd (indirect heating method).

ing method. At high temperatures and low pressures (reaction-I), the diffusion of the decomposed intermediate in the hydrogen sheath over the substrate is the rate-limiting step of the pyrolytic graphite formation. At low temperatures and low pressures (reaction-II), the rate-limiting step is the decomposition of a parent hydrocarbon gas molecule. At high pressures over a wide temperature range (reaction-III), since the complex reactions in the vapour phase are overlapped, the rate-limiting step is not definitely explained. These three types of the formation mechanism and the cause of the occurrence of a minimum density are qualitatively related to the structural features. In figs. 10a to 10d, the temperature for the change in the formation mechanism and for the occurrence of a minimum density are represented as "M" and "D" respectively. Below the temperature of "D", L_a is constant and independent of temperature. Above "D", L_a increases with temperature. On the other hand, L_c increases with temperature below the temperature of "M", but is independent of the increasing temperature above "M".

The processes of formation and development of the crystallite of pyrolytic graphite from hydrocarbon by thermal decomposition are considered to occur as shown in fig. 13. A parent hydrocarbon gas forms a radical containing a small amount of hydrogen by way of dehydrogenation and polymerisation. The radical forms a flat polymer through further dehydrogenation and polymerisation, which still contains a considerable amount of hydrogen. The flat polymer forms a crystallite nucleus of size 60 to 70 Å cube by further repetitions of dehydrogenation and polymerisation; the nucleus still contains an appreciable amount of hydrogen. The nucleus deposits on the heated substrate and forms a crystallite.

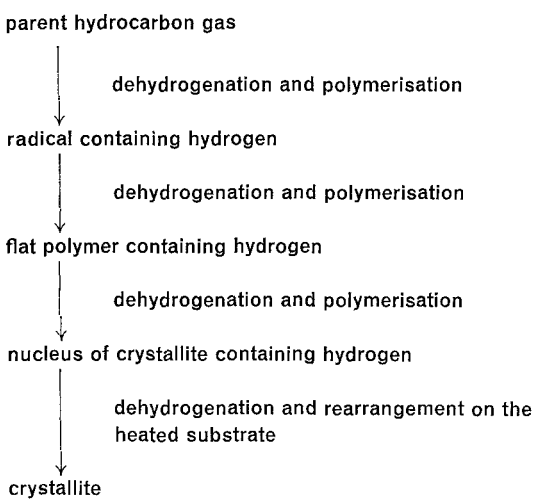

Figure 13 The processes of formation and development of the crystallite from hydrocarbon gas.

At high temperatures and low pressures (reaction-I), the concentration of hydrogen contained in the radical, flat polymer, and nucleus becomes very low, and the relative abundance of the radical to other products becomes very high. Therefore, in the nucleus, a large quantity of the radical sticks, in such a way as to envelop the nucleus, resulting in rapid development of the nucleus. The development of the carbon hexagon network proceeds in the *a* and *b* directions, so that the development of L_a is remarkable, but L_c does not increase.

At medium temperatures and low pressures, the radical and nucleus also exist, but the abundance of the flat polymer is more than those of the radical and nucleus. Therefore, the flat polymer sticks to the nucleus containing hydrogen, deposited in a rough state on the heated substrate. In this case, there is no rearrangement of crystallite by dehydrogenation after deposition, and therefore the density becomes lowered and preferred orientation of deposit deranged.

At low temperatures and low pressures (reaction-II), the abundance of the nucleus containing hydrogen is remarkable, and the radical containing hydrogen sticks to the nucleus. In this case, the rearrangement occurs with the dehydrogenation of the nucleus and radical after deposition, followed by the increases in density and preferred orientation. These features are shown in fig. 14. Since gas pressure does not affect the relative abundance of each intermediate, under high-pressure conditions such as 50 and 100 torr it is considered that the process of the development of crystallite is similar to that of the low-pressure conditions. Under the high-pressure conditions, however, it is evident from the soot formation in the vapour phase that there are large numbers of the nucleus, radical, and flat polymer particles in the vapour phase. It seems that the rearrangement of deposited crystallites on the heated substrate by heat treatment occurs only with difficulty owing to a faster deposition rate compared with low pressures. It follows that the preferred orientation of the deposit obtained at

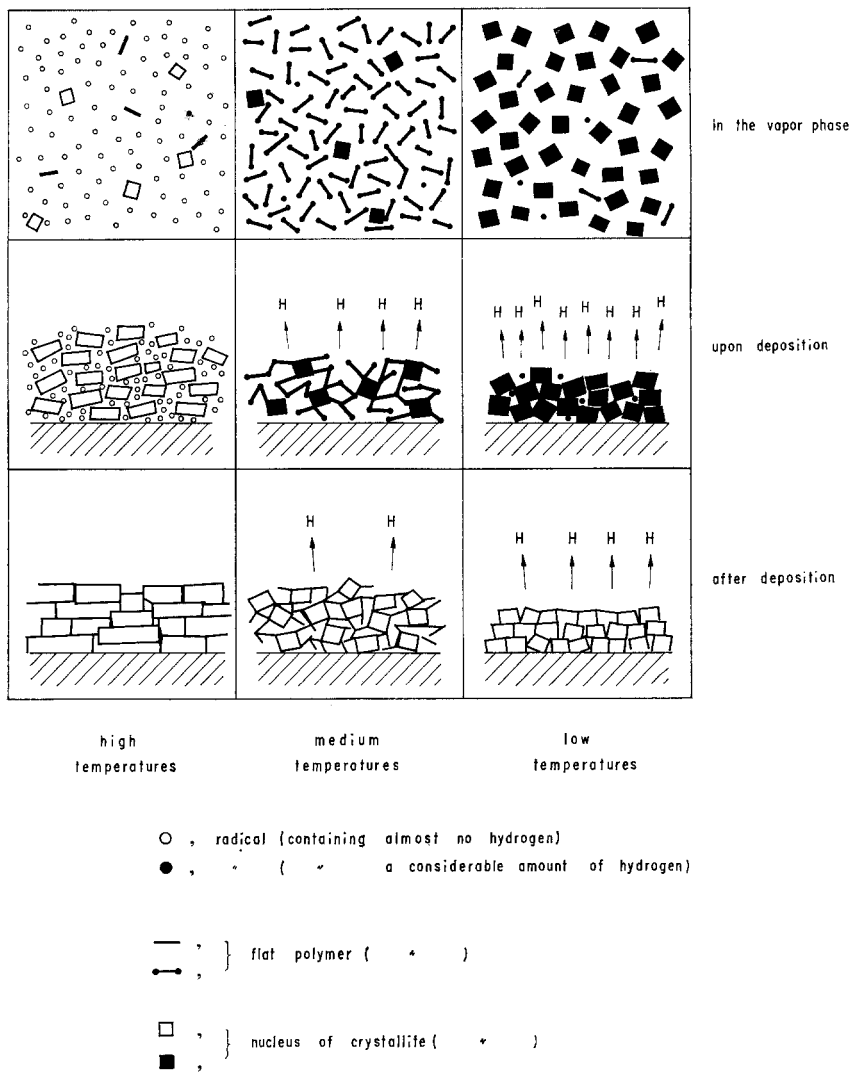

Figure 14 Schematic diagram of pyrolytic graphite formation.

high pressures is reduced in comparison with that at low pressures.

5. Conclusions

(*a*) The relation between interlayer spacing of pyrolytic graphite and deposition temperature is very complex, and the effect of temperature varies with pressure.

(*b*) The fine, regenerative (F) structure is obtained in the phase in which the interlayer spacing decreases with increasing temperature, and the coarse (C), pebble (P), and string (S) structures are obtained in the phase which shows an abnormal behaviour of the interlayer spacing with temperature.

(*c*) The intercrystallite porosity reaches a maximum value of 40 to 45% at the temperature at which a minimum density is obtained.

(*d*) The amount of ordering is closely related to the microstructure. The ordering is observed only in the structure "F", except that obtained at 5 torr.

(*e*) The anisotropy factor is generally small and becomes remarkably lower at low temperature and high pressure. It increases with temperature in the regions of "P" and "S", but in the region of "F" it is practically constant and independent of temperature.

(*f*) The relation of the crystallite sizes to deposition temperature shows a characteristic be-

haviour under various conditions and is closely related to the mechanism of pyrolytic graphite formation.

Acknowledgements

The authors wish to express their appreciation to Mr Kōichi Saito for his assistance in the preparation of various specimens and to Mr Yoshiharu Chiba for his cooperation throughout the experiments.

References

1. S. YAJIMA, T. SATOW, and T. HIRAI, *J. Nucl. Mat.* **17** (1965) 116.
2. *Idem, ibid*, 127.
3. Japan Society for the Promotion of Science (JSPS), Carbon No. 36 (1963) 25.
4. G. E. BACON, *J. Appl. Chem.* **6** (1956) 477.
5. S. YAJIMA and T. HIRAI, JSPS, 117-88-C-1, to be published.
6. O. J. GUENTERT, *J. Chem. Phys.* **37** (1962) 884.
7. T. NODA, M. INAGAKI, H. KATŌ, and M. TANAKA, *J. Chem. Soc. of Japan*, Ind. Chem. Sec. **65** (1962) 463.
8. A. G. R. BROWN and W. WATT, *Proc. Conf. on Ind. Carbon and Graphite*, Soc. Chem. Ind., London (1958) 86.
9. L. C. F. BLACKMAN and A. R. UBBELOHDE, *Proc. Roy. Soc.*, London **266** (1962) 20.
10. A. W. MOORE, A. R. UBBELOHDE, and D. A. YOUNG, *Brit. J. Appl. Phys.* **13** (1962) 393.
11. O. J. GUENTERT and C. T. PREWITT, *Bull. Amer. Phys. Soc.* **5** (1960) 187.
12. L. C. BLACKMAN, G. SAUNDERS, and A. R. UBBELOHDE, *Proc. Roy. Soc.* **A264** (1961) 19.
13. R. H. BRAGG, M. L. HAMMOND, J. C. ROBINSON, and P. L. ANDERSON, *Nature* **200** (1963) 555.
14. J. O. STIEGLER, C. K. H. DUBOSE, and J. L. COOK, *7th Conf. on Carbon*, Cleveland (1965).
15. E. R. STOVER, GE Report No. 62-RL-2564M (1960).
16. A. G. R. BROWN, D. CLARK, and J. EASTBROOK, *J. Less-Common Met.* **1** (1959) 94.
17. J. C. BOKROS, *Carbon* **3** (1965) 201.
18. A. R. UBBELOHDE, D. A. YOUNG, and A. W. MOORE, *Nature* **193** (1962) 571.